PRIMARY RESEARCH ARTICLE

Disproportionate microbial responses to decadal drainage on a Siberian floodplain

Min Jung Kwon[1] | Binu M. Tripathi[1] | Mathias Göckede[2] | Seung Chul Shin[1] | Nu Ri Myeong[1] | Yoo Kyung Lee[1] | Mincheol Kim[1]

[1]Korea Polar Research Institute, Incheon, Republic of Korea

[2]Max Planck Institute for Biogeochemistry, Jena, Germany

Correspondence
Mincheol Kim, Korea Polar Research Institute, Incheon 21990, Republic of Korea.
Email: mincheol@kopri.re.kr

Present address
Min Jung Kwon, Le Laboratoire des Sciences du Climat et de l'Environnement, Gif-sur-Yvette, 91191, France

Abstract

Permafrost thaw induces soil hydrological changes which in turn affects carbon cycle processes in the Arctic terrestrial ecosystems. However, hydrological impacts of thawing permafrost on microbial processes and greenhouse gas (GHG) dynamics are poorly understood. This study examined changes in microbial communities using gene and genome-centric metagenomics on an Arctic floodplain subject to decadal drainage, and linked them to CO_2 and CH_4 flux and soil chemistry. Decadal drainage led to significant changes in the abundance, taxonomy, and functional potential of microbial communities, and these modifications well explained the changes in CO_2 and CH_4 fluxes between ecosystem and atmosphere—increased fungal abundances potentially increased net CO_2 emission rates and highly reduced CH_4 emissions in drained sites corroborated the marked decrease in the abundance of methanogens and methanotrophs. Interestingly, various microbial taxa disproportionately responded to drainage: *Methanoregula*, one of the key players in methanogenesis under saturated conditions, almost disappeared, and also *Methylococcales* methanotrophs were markedly reduced in response to drainage. Seven novel methanogen population genomes were recovered, and the metabolic reconstruction of highly correlated population genomes revealed novel syntrophic relationships between methanogenic archaea and syntrophic partners. These results provide a mechanistic view of microbial processes regulating GHG dynamics in the terrestrial carbon cycle, and disproportionate microbial responses to long-term drainage provide key information for understanding the effects of warming-induced soil drying on microbial processes in Arctic wetland ecosystems.

KEYWORDS
CO_2 and CH_4 flux, long-term drainage, metagenome-assembled genomes, methanogens, permafrost thaw, soil microbiome

1 | INTRODUCTION

Global air temperature has risen over the past few decades, and the increasing trend is stronger than average in the Arctic (Huang et al., 2017; Serreze & Barry, 2011). Arctic warming may thaw permafrost—perennially frozen soil layers—and melt ground ice, which prevalently exists across the Arctic (Schirrmeister et al., 2002, 2013); furthermore, the subsequent carbon (C) release from previously frozen soil layers implies that this additional CO_2 emission to the atmosphere can contribute a stronger positive feedback to global warming temperatures (Hicks Pries et al., 2016; Schuur et al., 2009; Strauss et al., 2017). Higher temperature increases

Min Jung Kwon and Binu M. Tripathi should be considered joint first authors.

decomposition rates of carbon stored in soils (Bond-Lamberty & Thomson, 2010; Davidson & Janssens, 2006; Walker et al., 2018). Additionally, melting of bulk ice is followed by geomorphological changes and surface water redistribution (Aas et al., 2019; Avis et al., 2011; Liljedahl et al., 2016), and this changing soil hydrology between dry and wet conditions adds complexity in estimating the amount and forms of released C (Schädel et al., 2016; Schuur et al., 2015): wetter soil condition after permafrost thaw, such as development of thermokarst features and bogs (Osterkamp et al., 2009; Rodenhizer et al., 2020), decreases CO_2 but increases CH_4 emissions (Johnston et al., 2014; McCalley et al., 2014), whereas drier soil conditions increase CO_2 but decrease CH_4 emissions (Kittler et al., 2017; Lawrence et al., 2015), which is potentially counterbalancing the effect of preserving old C by impeding permafrost thaw (Kwon et al., 2019).

Compared to the warming–wetting effects on biogeochemical processes in the Arctic (e.g., Farquharson et al., 2019; McCalley et al., 2014; Olefeldt et al., 2016), less attention has been paid to warming–drying effects. Certain studies have examined drying effects on greenhouse gas (GHG) fluxes, vegetation, and soil chemistry in the Arctic (van der Kolk et al., 2016; Ward & Cory, 2015; Zona et al., 2009); however, although microorganisms play a pivotal role in regulating biogeochemical processes such as C decomposition and GHG dynamics, drying effects on microbial communities and functions, and their relationships to the GHG fluxes remain largely unexplored in the Arctic. A recent study found that microtopographic features of polygonal tundra that regulate the soil water distribution affect the structure and function of soil microbial communities (Taş et al., 2018). Comparing naturally wet and dry ecosystems can be a direct and clear way to investigate soil hydrological effects. A natural gradient in soil hydrology can form gradually or abruptly (especially following permafrost thaw, e.g., Olefeldt et al., 2016), and lacking the knowledge of the exact hydrological history can be a challenge for accurate evaluation. An artificial drainage experiment enables us to trace the changes in characteristics and functions from the start of the differential soil hydrology and to examine the important relationships between soil hydrology and ecosystem properties. To date, the only study that examined the impact of long-term artificial drainage on soil microbial communities found potential links between CH_4 fluxes and CH_4-related microorganisms; that is, a decline in the population size of methanogenic and methanotrophic taxa was accompanied by a corresponding reduction in the fluxes of CH_4 following drainage (Kwon et al., 2017). However, this previous study provides only a preliminary and partial insight into the taxonomic structure of microbial communities, as it analyzed only one replicate per treatment using partial 16S rRNA gene sequencing. In this study, we examined microbial communities of soil profiles (six replicates each from drained and undrained control sites) by pairing amplicon sequencing (16S rRNA gene) with shotgun metagenomic sequencing, which allows a more comprehensive understanding of the functional and genomic attributes of microbial communities.

Furthermore, we used a genome-centric approach to reveal the functional potential and abundance of metagenome-assembled genomes (MAGs), which leads to a more detailed understanding of novel metabolic pathways and microbial interactions among co-occurring taxa.

To identify key microbial functions and taxonomic groups associated with drainage-induced changes in CO_2 and CH_4 dynamics and soil biochemistry, we compared the soil microbial communities between drained and control plots at a decade-long experimental drainage manipulation site on a floodplain in the Siberian Arctic. Microbial group-specific quantitative polymerase chain reaction (qPCR) assays were performed, and shotgun metagenomic sequencing was employed for in-depth assessment of the drainage-induced changes in microbial taxa and functions at the population level, and to link them to microbe-derived CO_2 and CH_4 emissions. Considering that drainage effects are more noticeable within the surface layers, the comparison was primarily made at two organic soil depths: surface layer (0–7.5 cm) and subsurface layer (7.5–15 cm). First, we hypothesize that decadal drainage will result in more pronounced shifts in microbial communities at the surface layer than the subsurface layer because the deepened water table (WT) in drained plots reduces the total inundation period and frequency, which makes the surface soils more oxic. Second, the abundance of methanogens, as well as methanotrophs, will decrease due to the oxic condition following drainage, which inhibits CH_4 production and reduces CH_4 availability to be oxidized. Furthermore, various taxa may respond differently to the drainage due to their distinct physiological traits; we attempted to identify the microbial taxa showing a disproportionate response to the drainage.

2 | METHODS

2.1 | Study site

The study site (Göckede et al., 2019) is located on a floodplain of the Kolyma River near Chersky in northeastern Siberia. The mean annual temperature within the period 1960–2009 was −11°C, with monthly mean values ranging between −33 and +12°C (Göckede et al., 2017). The average annual precipitation (1950–1999) was 197 mm (Göckede et al., 2017). Due to snowmelt at the site and flooding from the nearby river basin, in most years the water level at the site increases up to 50 cm above the soil surface between May and early June and decreases gradually from mid-June to mid-July. Tussock-forming sedges, *Carex appendiculata* and *Carex lugens*, and cotton sedges, *Eriophorum angustifolium*, are the dominant plant species. An organic peat layer (15–25 cm) was placed on top of silty clay alluvial materials.

One subsection of the study site has been drained since 2004, which lowered the WT during the growing seasons (drained site; 68.6131 N, 161.3414 E), whereas the other site has not been manipulated (control site; 68.6167 N, 161.3497 E). The two sites start

with a similar WT during the flooding/snowmelt season, but the drainage ditch renders distinctively low WT at the drained site over the growing season—the WT of the drained site decreases up to ca. 20 cm, while that of the control site is maintained at the soil surface (Kwon et al., 2016). Due to this difference, both surface and subsurface layers of the control site were inundated from snowmelt until the time of soil sampling (July 31); however, surface layers of the drained site were continuously dry from July 1 to 31, whereas subsurface layers experienced partially wet conditions. The two sites are located approximately 600 m away from each other (Figure S1). Within each of these two sites, we took soil samples from six plots at 50-m intervals. Owing to the heterogeneous topography within sites, one plot at the control site showed lower WT similar to that of the drained site (defined as control-dry), and one plot at the drained site presented higher WT similar to that of the control site (defined as drained-wet). We primarily focused on the comparison between control-wet and drained-dry plots, thus control sites refer to control-wet and drained sites refer to drained-dry for simplicity when not specified. Additionally, we included control-dry and drained-wet in the analysis to compare the effects of 10 years of drainage and natural variation of WT depth (>10 years) on microbial communities as well as CO_2 and CH_4 fluxes. This information backs up the lack of information for the initial condition at the start of the manipulation experiment and indicates whether long-term WT manipulation can represent natural WT variations.

2.2 | Heterotrophic respiration (R_h) and CH_4 flux rates

For the present work, we used CO_2 and CH_4 flux data of 2014 from Kwon et al. (2016, 2017, and 2019), and the methods used are described briefly as follows. CO_2 and CH_4 fluxes were measured at one plot per treatment over the growing season of 2014 ($n = 4$). These locations were selected considering the dominant plant species (e.g., *E. angustifolium* and shrub species for wet, and *C. appendiculata* and *E. angustifolium* for dry) and WT conditions (e.g., WT close to the soil surface for wet, and WT below 10 cm for dry; Kwon et al., 2016, 2017) per treatment. The selected plots showed CO_2 flux rates close to the average of each treatment (Kwon et al., 2016), and highest and lowest range of CH_4 fluxes (Kwon et al., 2017) of all plots at each treatment. We estimated R_h within the surface layer (0–15 cm) and all deeper soil layers (up to the thaw depth at the time of soil sampling) by multiplying the measured ecosystem respiration (Kwon et al., 2016) with the R_h proportion in the surface layer (control-wet: 25.2%, drained-dry: 56.4%, control-dry: 53.8%, and drained-wet: 38.0%) and all soil layers (control-wet: 75.9%, drained-dry: 65.5%, control-dry: 67.8%, and drained-wet: 63.0%) as described in Kwon et al. (2019). We adopted daily CH_4 flux rates from Kwon et al. (2017). More details can be found in the Method S1 and Kwon et al. (2016, 2017, and 2019).

2.3 | Soil sampling and soil chemistry

Six soil cores (diameter of 7.6 cm) were collected from each site in July 2014. Each core was divided into an organic peat layer (15 cm on average) and an alluvial soil layer, and thereafter, each layer was further divided into 7.5-cm increments in order to secure sufficient amounts of soils for chemical and molecular analyses. We used the top 15 cm of the organic peat layer for the analysis since DNA concentrations of mineral soils were too low to generate metagenomic sequencing libraries. All the surface soils were collected from 0 to 7.5 cm depths, and subsurface soils were from 7.5 cm up to 10.5–18 cm depths (on average 15 cm depth). After removing roots (>1 mm diameter), soils were gently mixed within the sample bags for homogenization. For microbial analysis, the soil subsamples were kept in a preservation solution (reagent made following the recipe of RNAlater, which precipitates cellular proteins including RNase; Salehi and Najafi (2014) and frozen at −20°C until further analyses.

The soil subsamples were dried at 105°C for 24 h to determine the gravimetric soil moisture content (%). Total carbon and nitrogen percentages were estimated by an elemental analyzer (Vario EL, Elementar) after drying peat soils at 70°C. Soil pH was measured by mixing soil and distilled water in a 1:1 ratio. Water-soluble nitrogen (nitrate, nitrite, and ammonium) was extracted by mixing soils with 1 M KCl solution in a 1:10 ratio and shaking them for 1 h. Thereafter, the concentrations of nitrate, nitrite, and ammonium were assessed by using a continuous flow meter (QuickChem 8500; Lachat). To extract sulfate from the soil, air-dried soils were mixed with calcium phosphate solution (500 mg phosphate L^{-1}) in a 1:2.5 (for mineral soils) and 1:5 ratio (for organic peat soils), shaken for 30 min and filtered through Whatman quantitative filters. The sulfate concentration of the filtrate was determined via ion chromatography (DX-500; Dionex).

2.4 | qPCR for fungi, archaea, and bacteria

Soil DNA was extracted from 2 g of each soil sample using a PowerSoil Total DNA Isolation Kit (MO BIO Laboratories) according to the manufacturer's instructions. DNA with high humic acid content was further purified using a PowerClean Pro DNA Clean-Up kit (MO BIO Laboratories). qPCR was performed on a Rotor-Gene Q thermal cycler (QIAGEN) using SYBR Green Supermix (Bio-Rad) to measure abundances of fungi, bacteria, and archaea. All details about primers and PCR conditions are provided in the Suppoting Information.

2.5 | Amplicon sequencing and community analyses

The purified genomic DNA was sent to the Integrated Microbiome Resource (IMR; http://cgeb-imr.ca) for library construction and MiSeq amplicon sequencing (2 × 300 bp). All details about custom

fusion primers, library preparation, and sequencing have been described previously (Comeau et al., 2017). Briefly, DNA was amplified by targeting three microbial groups (V4–V5 regions of bacterial and archaeal 16S rRNA gene or eukaryotic 18S rRNA gene, V6–V8 regions of archaeal 16S rRNA gene). Raw reads were processed following the MiSeq SOP in mothur v1.44.1 (Schloss et al., 2009). Furthermore, high-quality sequences were taxonomically assigned to genus-level phylotypes against the EzBiocloud database (May 2018; Yoon et al., 2017) for bacteria and archaea using the Naïve Bayesian Classifier with a confidence threshold of 80%. Quality-filtered sequences were clustered into operational taxonomic units (OTUs) at a 97% similarity cutoff, and singleton OTUs were omitted to avoid sequencing bias in the following community analyses.

2.6 | Shotgun metagenome sequencing

Metagenomic sequencing libraries were constructed using a TrueSeq Nano DNA Library Prep kit, and then QC passed libraries were sequenced at Macrogen Incorporation using an Illumina HiSeq 4000 (2 × 150 bp). Sequencing adapters and low-quality reads were filtered out using Trimmomatic v0.39 with default settings (Bolger et al., 2014). QC passed reads were searched against NCBI-nr DB (downloaded in May, 2019) using a DIAMOND v0.9.10.111 blastx aligner with default parameters (Buchfink et al., 2015), and the resultant-aligned reads were mapped to the Kyoto Encyclopedia of Genes and Genomes (KEGG) mapping files in MEGAN6 Ultimate Edition v6.5.7 (Huson et al., 2007). Metagenomic coverage and sequence diversity of samples were estimated using Nonpareil v3.304 (Rodriguez-R et al., 2018). rRNA gene fragments (16S and 28S rRNA genes) were extracted from metagenomic data using SortMeRNA v2.1b (Kopylova et al., 2012), and Hidden Markov Model-searched read counts were used to estimate the bacterial, archaeal, and fungal abundances. To obtain more accurate phylogenetic information of methyl coenzyme M reductase (*mcrA*), particulate methane monooxygenase (*pmoA*), and soluble methane monooxygenase (*mmoX*) genes, the metagenomic reads were searched against *mcrA*-, *pmoA*-, and *mmoX*-specific packages (gpkgs) using GraftM program v0.11.1 (Boyd et al., 2018).

2.7 | Metagenome assembly, binning, and annotation

We combined two approaches for metagenome assembly as described previously (Stewart et al., 2018). Details about assembly, binning, and classification are provided in the Methods S1. Annotation for MAGs was performed by assigning KO (KEGG Orthology) identifiers to individual genes using BlastKOALA algorithm, and ambiguous annotations were further confirmed by performing BLASTP searches against the NCBI-nr database. For functional enrichment analysis across MAGs, we applied "anvi-compute-functional-enrichment"

using COG functions and KEGG modules in Anvi'o pangenomics workflow (Shaiber et al., 2020).

2.8 | Statistical analyses

A two-way ANOVA was performed to investigate the variations in gas fluxes, soil chemical properties, microbial abundances, α-diversity indices, and taxonomic and functional distributions of microbial communities based on treatment (control-wet vs. drained-dry) and soil depth (surface 0–7.5 cm vs. subsurface 7.5–15 cm). Tukey's post hoc test was successively performed. The OTU abundance data was Hellinger-transformed, and nonmetric multidimensional scaling (NMDS) plots were used to visualize the pairwise Bray–Curtis dissimilarities between communities. Two-way permutational multivariate ANOVA (PERMANOVA) was performed using the "adonis" function in R package "vegan" to determine whether the taxonomic and functional compositions of microbial communities differed according to the treatment and depth. Linear least-squares regression was performed to describe the relationship between the relative abundances of individual MAGs. All statistical analyses were performed in R software environment v.3.6.2 (R Development Core Team, 2013).

3 | RESULTS

3.1 | CO_2 and CH_4 fluxes and soil chemistry

Heterotrophic respiration rates within the surface layers (0–15 cm) from mid-June to mid-August 2014, which includes the peak growing season, were significantly higher in drained sites compared to those in control sites (control-wet: 0.63 ± 0.15, drained-dry: 1.73 ± 0.46 g C-CO_2 m^{-2} day^{-1}; $t = 17.76$, $p < 0.001$; Figure 1a). When R_h of all soil layers were compared, however, R_h rates in the drained sites were only 6.4% higher than those in the control sites (control-wet: 1.89 ± 0.47, drained-dry: 2.01 ± 0.54 g C-CO_2 m^{-2} day^{-1}), and the difference was not statistically significant ($t = 1.33$, $p > 0.05$; Figure 1a; shown in Kwon et al., 2016 and 2019). CH_4 flux rates were significantly lower at the drained plot, revealing a slight net CH_4 uptake, that is, CH_4 oxidation exceeded the CH_4 production (control-wet: 331.78 ± 168.30, drained-dry: -1.14 ± 1.58 mg CH_4 m^{-2} day^{-1}; $t = -15.58$, $p < 0.001$; Figure 1b; shown in Kwon et al., 2017). Control-dry showed similar Rh 0–15 cm and CH_4 fluxes to those of drained-dry, and drained-wet showed the flux ranges between those of control-wet and drained-dry (Figure 1a,b).

Although the WT was ca. 20 cm lower at the drained plots (control-wet: 2.89 ± 2.34, drained-dry: -18.58 ± 3.43 cm), gravimetric soil water content (%) differed neither by treatment nor by depth (ANOVA: all $p > 0.05$; Table 1). Total C and N contents (%) were significantly higher in the drained sites than in the control sites, but did not differ by depth (for both C and N: treatment $p < 0.01$, depth, treatment × depth $p > 0.05$). The C:N ratio and soil pH differed
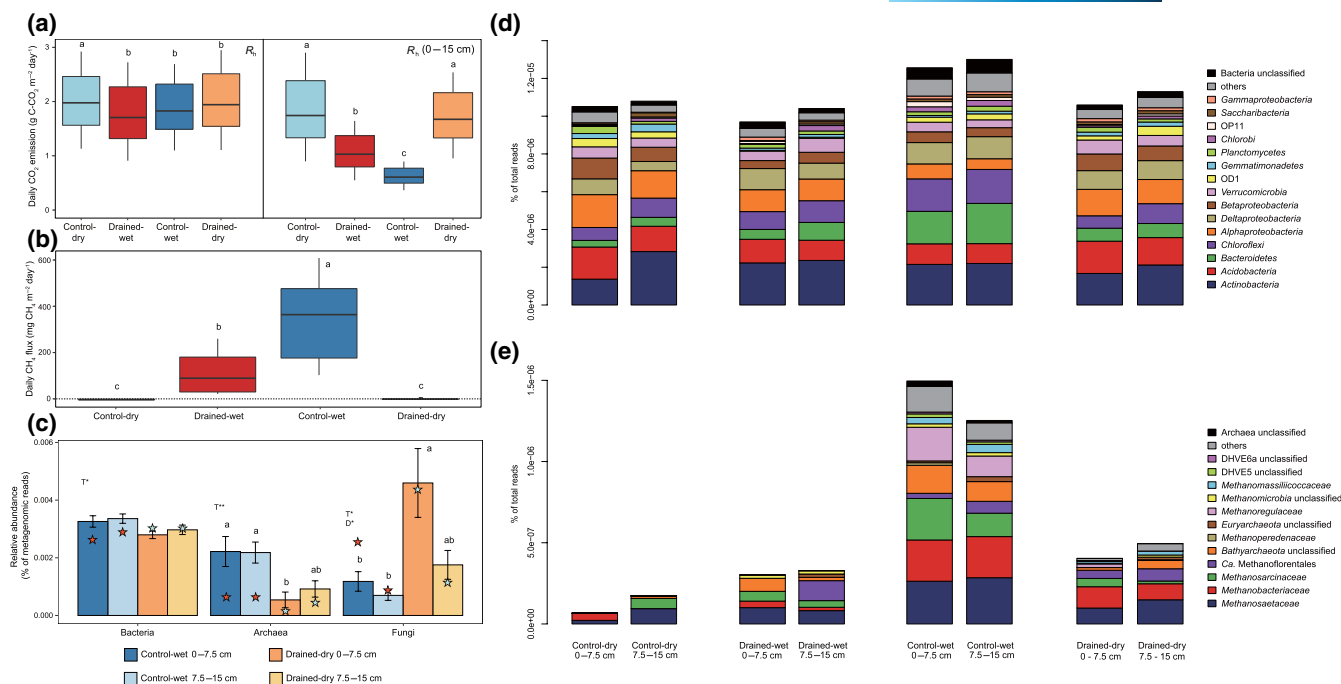
FIGURE 1 CO_2 and CH_4 flux, and the abundance and taxonomy of microbial communities based on metagenome-extracted rRNA fragment information. (a) Heterotrophic respiration (R_h) rates measured as total and at 0–15 cm depth. (b) Daily CH_4 flux rates, with negative CH_4 flux rates, indicating CH_4 oxidation rates exceed CH_4 production rates. (c) Sequence-based abundances of bacterial, archaeal, and fungal rRNA gene fragments (16S and 28S rRNA genes). (b, c) Boxplots denote first and third quartiles with median values, and whiskers represent 1.5*inter-quartiles. Star shapes on bar plot indicate data points of drained-wet (marginally influenced by drainage; red) and control-dry (naturally dry due to higher soil topography; light blue) treatments. T, treatment; D, soil depth. p-values are indicated by asterisks **$p < 0.01$, ***$p < 0.001$. Different letters indicate significant ($p < 0.05$) differences between groups. Mean relative abundance of (d) bacterial and (e) archaeal taxa according to treatment and depth. Bacterial and archaeal lineages are represented at the phylum level (or class level in the case of *Proteobacteria*) and family level, respectively

neither by treatment nor by depth (all $p > 0.05$). The amount of extractable sulfate revealed no difference by treatment but differed by depth (depth $p < 0.05$, treatment, treatment × depth $p > 0.05$), whereas the amount of extractable ammonium was slightly reduced in the drained sites, compared to the control sites (all $p > 0.05$). The amount of extractable nitrite was significantly reduced in the drained site (treatment $p < 0.01$, depth, treatment × depth $p > 0.05$); however, the amount of extractable nitrate was higher in the drained sites than in the control sites (treatment $p < 0.001$, depth, treatment × depth $p > 0.05$). More details of soil chemistry information are available in Table S1.

3.2 | Microbial abundance, diversity, and community composition

We used microbial relative abundance estimated from metagenome-derived 16S and 28S rRNA gene sequences for comparisons between treatments (Figure 1c). In comparison to the control sites, both bacterial and archaeal relative abundances were significantly reduced in the drained sites at both soil depths (all $p < 0.05$), but the extent of abundance decrease between these two taxonomic groups was different. Drainage led to a marked decrease in the relative

abundance of archaea (from 0.0022 ± 0.0010 to 0.0005 ± 0.0006 in the surface layer, and from 0.0022 ± 0.0007 to 0.0009 ± 0.0006 in the subsurface layer), whereas there was only a slight drainage-induced decrease in the relative abundance of bacteria at both depths (from 0.0033 ± 0.0004 to 0.0028 ± 0.0003 in the surface layer, and from 0.0034 ± 0.0003 to 0.0030 ± 0.0004 in the subsurface layer). Contrary to the results of prokaryotes, drainage resulted in a significant increase in the relative abundance of fungi at both soil depths (all $p < 0.05$). The drainage-induced increase in the relative abundance of fungi was more pronounced in the surface layer (from 0.0012 ± 0.0007 to 0.0046 ± 0.0027) than in the subsurface layer (from 0.0007 ± 0.0003 to 0.0018 ± 0.0011). To verify the results based on abundance estimates obtained from metagenome-derived rRNA gene sequences, we further performed comparisons between treatments using qPCR-based microbial abundance estimates. The qPCR-derived relative abundance of bacteria, archaea, and fungi showed overall similar trends to the metagenome-derived results, but there were larger variations in abundance values within each treatment group due to the high sensitivity of qPCR assay (Figure S2a).

Soil bacterial and functional α-diversity did not differ significantly following drainage ($p > 0.05$; Figure S2b), but were significantly influenced by depth, with a higher α-diversity consistently observed

TABLE 1 Mean and standard deviations of soil chemistry by treatment and soil depth. Data related to nitrogen (N) are collected in 2013, at the same locations as in 2014

	Control-dry		Drained-wet		Control-wet		Drained-dry		Two-way ANOVA
	Surface 0–7.5 cm	Subsurface 7.5–15 cm	Surface 0–7.5 cm	Subsurface 7.5–15 cm	Surface 0–7.5 cm	Subsurface 7.5–15 cm	Surface 0–7.5 cm	Subsurface 7.5–15 cm	
Gravimetric soil moisture content (%)	55.6	48.82	56.35	50.63	58.39 ±7.22	50.75 ±10.82	58.49 ±3.95	50.09 ±18.71	$T^{n.s.}, D^{n.s.}; T \times D^{n.s.}$
Total carbon (%)	27.4	25.65	35.01	34.89	22.82 ± 5.49^{b}	25.48 ± 3.59^{ab}	34.80 ± 2.99^{a}	31.98 ± 8.15^{ab}	$T^{**}, D^{n.s.}; T \times D^{n.s.}$
Total nitrogen (%)	1.66	1.49	1.85	2.00	1.42 ± 0.35^{b}	1.64 ± 0.25^{ab}	2.06 ± 0.09^{a}	1.94 ± 0.41^{ab}	$T^{**}, D^{n.s.}; T \times D^{n.s.}$
C:N	16.48	17.22	18.92	17.46	16.11 ±0.94	15.61 ±0.72	16.87 ± 1.09^{a}	16.31 ±1.34	$T^{n.s.}, D^{n.s.}; T \times D^{n.s.}$
pH	4.57	4.58	5.40	4.80	4.71 ±0.10	4.67 ±0.12	4.94 ±0.25	4.68 ±0.10	$T^{n.s.}, D^{*}; T \times D^{n.s.}$
Sulfate (µg dry g^{-1})	95.89	46.60	103.03	44.71	90.80 ± 29.27^{ab}	82.46^{ab}	156.47 ± 71.20^{a}	59.09 ± 13.05^{b}	$T^{n.s.}, D^{*}; T \times D^{n.s.}$
Ammonium (µg dry g^{-1})	18.92	31.13	3.03	4.67	36.06 ±38.15	29.17 ±23.54	11.92 ±7.83	5.67 ±1.76	$T^{n.s.}, D^{n.s.}; T \times D^{n.s.}$
Nitrite (µg dry g^{-1})	0.00	0.00	3.79	0.00	0.93 ± 0.65^{ab}	1.37 ± 1.11^{b}	0.00 ± 0.00^{a}	0.00 ± 0.00^{a}	$T^{**}, D^{n.s.}; T \times D^{n.s.}$
Nitrate (µg dry g^{-1})	11.97	10.75	87.90	16.67	4.69 ± 5.44^{ab}	1.86 ± 3.72^{b}	16.06 ± 6.48^{a}	13.60 ± 4.86^{a}	$T^{***}, D^{n.s.}; T \times D^{n.s.}$

Note: Different subscript letters denote significant differences ($p < 0.05$) between groups based on ANOVA followed by Tukey's HSD test.

Abbreviations: D, soil depth; n.s., Nonsignificant (two-way ANOVA);T, treatment.

*$p < 0.05$,; **$p < 0.01$.; ***$p < 0.001$.

in the surface soil, compared to the subsurface soil irrespective of the drainage treatment ($p < 0.05$; Figure S2b). A marked reduction in archaeal α-diversity was observed only in the subsurface soils of the drained plots ($p < 0.01$; Figure S2b).

The relative abundance of the majority of dominant bacterial phyla varied between the treatments. Of these, *Bacteroidetes*, *Chloroflexi*, *Chlorobi*, and OP11 were dominant in the control plots, whereas *Acidobacteria*, *Alphaproteobacteria*, *Betaproteobacteria*, *Verrucomicrobia*, and *Gemmatimonadetes* were more abundant in the drained plots (Figure 1d; Table 2); however, the relative abundance of OD1 was significantly influenced by soil depth, while the impact of the drainage treatment was rather weak (Table 2). The dominant archaeal taxa also varied between treatments, with *Methanosaetaceae*, *Methanosarcinaceae*, *Methanoregulaceae*, and unclassified lineage of *Bathyarchaeota* more abundant in control plots (Figure 1e; Table 2). Furthermore, the dominant bacterial and archaeal taxa in the 16S rRNA gene amplicon sequence data revealed similar results with few variations (Table S2; Figure S3). The bacterial community composition was primarily structured by drainage treatment (PERMANOVA: Pseudo-$F = 7.39$, $R^2 = 0.30$, $p < 0.01$), and to a lesser extent by depth (Pseudo-$F = 2.47$, $R^2 = 0.10$, $p < 0.05$; Figure 2a). The archaeal community composition was also influenced by treatment (Pseudo-$F = 4.52$, $R^2 = 0.18$ $p < 0.01$; Figure 2b) but more strongly by depth (Pseudo-$F = 5.28$, $R^2 = 0.21$, $p < 0.01$). The NMDS ordination plot showed that bacterial, archaeal, and functional genes compositions within control-dry samples at the surface layer were placed more closely to those of drained-dry plots, whereas the drained-wet communities were located in the middle of drained-dry and control-wet communities (Figure 2).

3.3 | Potential metabolic functions of microbial communities

The functional gene (KEGG level 3) composition of communities differed significantly by treatment (PERMANOVA: Pseudo-$F = 7.92$, $R^2 = 0.31$, $p < 0.01$; Figure 2d), whereas functional α-diversity decreased significantly only with depth ($F = 7.48$, $p < 0.05$; Figure S2b). The relative abundance of functional genes encoding cellulases was significantly influenced by treatment, with reduced abundance in the drained plots (Figure S4a), whereas that of xylanases was differentially abundant by depth, with higher values in the surface soils (Figure S4b). Moreover, the genes involved in the degradation of simple carbohydrates, such as xylose, galactose, lactose, sucrose, mannose, and fructose, were significantly reduced by drainage (Figure S4b). The functional genes involved in acetogenesis and ethanol fermentation were influenced by both treatment and depth, with significantly higher abundance in control plots than in drained plots, and in subsurface soils than in surface soils (Figure S4c). The genes related to lactate fermentation varied only by treatment, with greater abundance in drained plots (Figure S4c).

When the species scores were plotted on the ordination space, the genes involved in CH$_4$ metabolism (methanogenesis

TABLE 2 Relative abundance of dominant bacterial and archaeal taxa detected in metagenome-derived 16S rRNA gene sequence data by treatment and soil depth

	Control-dry		Drained-wet		Control-wet		Drained-dry		Two-way ANOVA
	Surface 0–7.5 cm	Subsurface 7.5–15 cm	Surface 0–7.5 cm	Subsurface 7.5–15 cm	Surface 0–7.5 cm	Subsurface 7.5–15 cm	Surface 0–7.5 cm	Subsurface 7.5–15 cm	
Bacteria									
Acidobacteria	$1.70E^{-06}$	$1.34E^{-06}$	$1.25E^{-06}$	$1.07E^{-06}$	$1.09E^{-06} \pm 2.40E^{-07b}$	$1.05E^{-06} \pm 1.07E^{-07b}$	$1.71E^{-06} \pm 3.08E^{-07a}$	$1.45E^{-06} \pm 2.23E^{-07ab}$	T***
Bacteroidetes	$3.52E^{-07}$	$4.72E^{-07}$	$5.22E^{-07}$	$9.43E^{-07}$	$1.72E^{-06} \pm 7.26E^{-07ab}$	$2.13E^{-06} \pm 8.03E^{-07a}$	$6.88E^{-07} \pm 5.24E^{-07bc}$	$7.46E^{-07} \pm 8.91E^{-07ab}$	T**
Chloroflexi	$6.83E^{-07}$	$1.02E^{-06}$	$9.44E^{-07}$	$1.15E^{-06}$	$1.72E^{-06} \pm 4.37E^{-07a}$	$1.80E^{-06} \pm 2.09E^{-07a}$	$6.56E^{-07} \pm 4.08E^{-07b}$	$1.05E^{-06} \pm 5.81E^{-07ab}$	T***
Alphaproteobacteria	$1.74E^{-06}$	$1.45E^{-06}$	$1.16E^{-06}$	$1.15E^{-06}$	$7.92E^{-07} \pm 1.71E^{-07bc}$	$5.65E^{-07} \pm 9.80E^{-08c}$	$1.40E^{-06} \pm 2.13E^{-07a}$	$1.28E^{-06} \pm 4.31E^{-07ab}$	T***
Betaproteobacteria	$1.10E^{-06}$	$7.55E^{-07}$	$4.22E^{-07}$	$5.74E^{-07}$	$5.70E^{-07} \pm 1.12E^{-07b}$	$4.76E^{-07} \pm 1.03E^{-07b}$	$8.83E^{-07} \pm 2.19E^{-07a}$	$7.77E^{-07} \pm 2.69E^{-07ab}$	T***
Verrucomicrobia	$5.95E^{-07}$	$4.88E^{-07}$	$5.02E^{-07}$	$7.38E^{-07}$	$5.09E^{-07} \pm 1.14E^{-07ab}$	$4.16E^{-07} \pm 2.12E^{-07b}$	$7.38E^{-07} \pm 1.61E^{-07a}$	$5.57E^{-07} \pm 1.41E^{-07ab}$	T*
OD1	$4.40E^{-07}$	$3.30E^{-07}$	$4.02E^{-08}$	$6.15E^{-08}$	$2.65E^{-07} \pm 9.82E^{-08ab}$	$3.15E^{-07} \pm 1.59E^{-07ab}$	$2.22E^{-07} \pm 7.88E^{-08b}$	$4.86E^{-07} \pm 1.57E^{-07a}$	D*
Gemmatimonadetes	$2.64E^{-07}$	$4.09E^{-07}$	$1.20E^{-07}$	$1.44E^{-07}$	$9.09E^{-08} \pm 5.11E^{-08}$	$1.43E^{-07} \pm 1.08E^{-07}$	$1.97E^{-07} \pm 7.28E^{-08}$	$2.24E^{-07} \pm 3.74E^{-08}$	T*
Chlorobi	$4.40E^{-08}$	$1.73E^{-07}$	$4.02E^{-08}$	$2.87E^{-07}$	$2.63E^{-08} \pm 8.43E^{-08}$	$3.02E^{-07} \pm 9.99E^{-08}$	$8.42E^{-08} \pm 7.29E^{-08}$	$1.53E^{-07} \pm 1.82E^{-07}$	T*
OP11	$4.40E^{-08}$	$6.29E^{-08}$	$1.20E^{-07}$	$8.20E^{-08}$	$2.74E^{-07} \pm 7.46E^{-08a}$	$1.72E^{-07} \pm 3.26E^{-08ab}$	$6.21E^{-08} \pm 1.08E^{-07b}$	$1.14E^{-07} \pm 8.95E^{-08ab}$	T**
Archaea									
Methanosaetaceae	$2.20E^{-08}$	$9.44E^{-08}$	$1.00E^{-07}$	$8.20E^{-08}$	$2.63E^{-07} \pm 7.25E^{-08}$	$2.85E^{-07} \pm 9.07E^{-08}$	$9.80E^{-08} \pm 1.54E^{-07}$	$1.49E^{-07} \pm 1.15E^{-07}$	T*
Methanobacteriaceae	$4.40E^{-08}$	$0.00E^{+00}$	$4.02E^{-08}$	$2.05E^{-08}$	$2.54E^{-07} \pm 1.57E^{-07}$	$2.53E^{-07} \pm 1.58E^{-07}$	$1.31E^{-07} \pm 9.13E^{-08}$	$9.87E^{-08} \pm 6.77E^{-08}$	T*
Methanosarcinaceae	$0.00E^{+00}$	$6.29E^{-08}$	$6.02E^{-08}$	$4.10E^{-08}$	$2.56E^{-07} \pm 3.17E^{-07}$	$1.44E^{-07} \pm 7.26E^{-08}$	$5.11E^{-08} \pm 5.65E^{-08}$	$1.70E^{-08} \pm 2.67E^{-08}$	T*
Bathyarchaeota un.	$0.00E^{+00}$	$1.57E^{-08}$	$8.03E^{-08}$	$2.05E^{-08}$	$1.73E^{-07} \pm 8.10E^{-08a}$	$1.22E^{-07} \pm 9.59E^{-08ab}$	$1.66E^{-08} \pm 1.74E^{-08b}$	$5.14E^{-08} \pm 3.72E^{-08b}$	T**
Methanoregulaceae	$0.00E^{+00}$	$0.00E^{+00}$	$0.00E^{+00}$	$0.00E^{+00}$	$2.07E^{-07} \pm 9.58E^{-08a}$	$1.27E^{-07} \pm 8.19E^{-08ab}$	$2.21E^{-08} \pm 3.98E^{-08bc}$	$0.00E^{+00} \pm 0.00E^{+00c}$	T***

Note: Data represent mean ± SD.

Different subscript letters denote significant differences ($p < 0.05$, ANOVA, Tukey's HSD) between groups.

Abbreviations: D, soil depth; T, treatment.

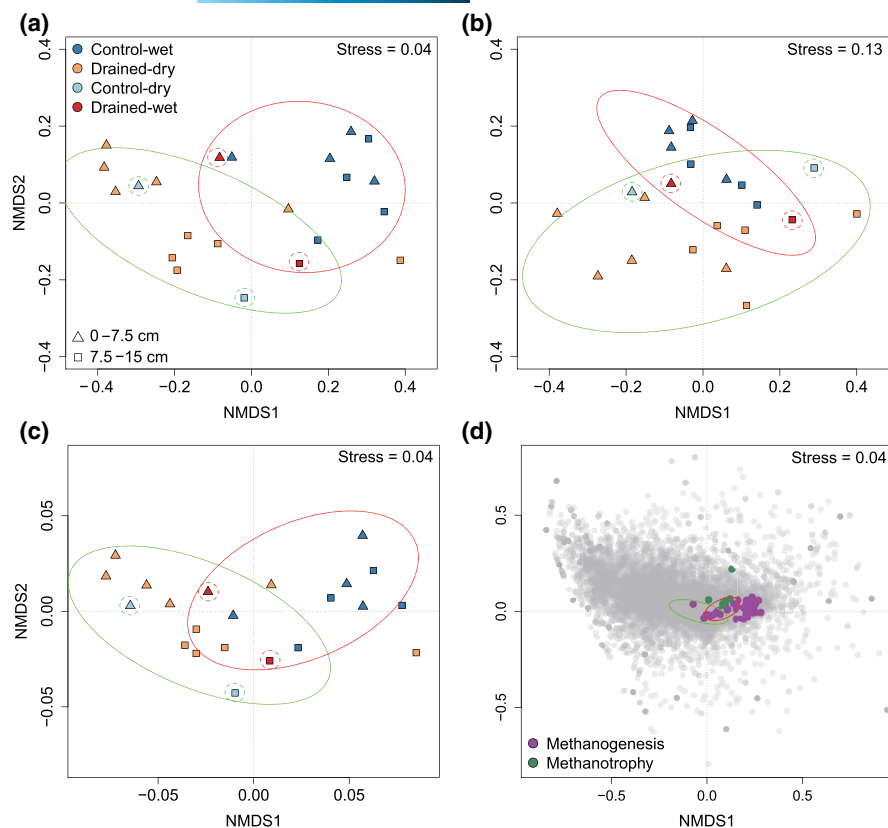*$p < 0.05$,; **$p < 0.01$,; ***$p < 0.001$ (two-way ANOVA).

FIGURE 2 Drainage-induced shifts in the taxonomic and functional compositions of microbial communities. Nonmetric multidimensional scaling (NMDS) ordination plot depicting changes in the composition of (a) bacterial and (b) archaeal communities, as well as (c) Kyoto Encyclopedia of Genes and Genomes (KEGG; level 3) functional genes among samples. Ordinations are based on Bray–Curtis dissimilarity (colors: treatment, shape: soil type), and ellipses indicate control-wet (red) and drained-dry (green) treatments. Samples encircled with dotted lines indicate control-dry (green) and drained-wet (red) treatments. (d) NMDS plot illustrating the species scores of KEGG functional genes with special reference to functional genes associated with methanogenesis and methanotrophy

and methanotrophy) were strongly enriched in the control plots (Figure 2d). The relative abundance of genes involved in methanogenesis from different pathways, including from CO_2, acetate, methanol, and methylamines, was reduced following drainage, except in one soil core of the drained plot (T1-10 in Figure 3a). Similarly, the genes encoding both particulate methane/ammonia monooxygenase (*pmoABC/amoABC*) and soluble methane monooxygenase (*mmoXYZ*), which are involved in methanotrophy, were also significantly decreased in the drained plots (Figure 3b). Taxonomic classification of methyl coenzyme M reductase (*mcrA*) reads revealed a diverse group of methanogens (Figure S5a), and their distributions were influenced by the treatment (Table S3). *Methanoregula* disappeared in drained plots and the abundance of certain other methanogenic genera such as *Methanosaeta*, *Methanobacterium*, and *Methanosarcina* was also decreased in the drained plots (Table S3). Similar to the 16S rRNA gene results, *Ca.* "Methanoflorentales" (taxonomic classification based on *mcrA* gene) were more abundant in the subsurface soils of both treatments (Figure S5a). The taxonomy of *pmoA* and *mmoX* reads revealed that the proportion of *Methylococcaceae pmoA* and *mmoX* was significantly reduced in drained plots, and *Methylocystaceae mmoX* was more abundant in the surface layer than in the subsurface layer, regardless of treatment (Figure S5b; Table S3). Upland soil cluster alpha (USCα) *pmoA* gene sequences showed a consistent abundance across almost all samples, irrespective of treatment and soil depth (Figure S5b).

The genes involved in assimilatory nitrate reduction increased in the drained plots, whereas those related to dissimilatory nitrate reduction were significantly reduced (Figure 3c). No significant changes were observed in the relative abundance of genes involved in denitrification, except *nirK* and *nosZ*, which were more abundant in the drained plots (Figure 3c). The relative abundance of most of the genes involved in assimilatory sulfate reduction was abundant in the drained plots, whereas those related to dissimilatory sulfate reduction were dominant in subsurface soils (Figure 3c). Furthermore, the relative proportion of genes involved in stress response, ABC transporters, and cytochrome c oxidase (aa$_3$- and cbb$_3$-type) was increased in the drained plots (Figures S6 and S7).

3.4 | MAGs and syntrophic associations

In total, 337.0 Gb of shotgun metagenomic sequence data were generated, with an average of 14.7 Gb per sample (Table S4), and the estimated metagenomic coverage ranged from 27.4% to 56.7% (38.5% on average). Metagenome assembly and binning yielded 119 high-quality nonredundant MAGs (110 bacteria and nine archaea), with an estimated quality score of ≥60 (defined as completeness – 5 × contamination) and dereplication at ≥95% ANI cutoff (Table S5). When the resultant MAGs were placed in an archaeal genome tree, eight archaeal MAGs were identified as novel lineages above the species level. A *Methanoregula* MAG (Chersky.34_13), whose abundance was markedly reduced following drainage, was closely related to the Stordalen mire MAG (GCA_003154335; 97.2% ANI; Figure 4a). A novel *Ca.* "Methanoflorentales" MAG (Chersky.15_44), which is consistently abundant in the deeper layers of both treatments, is
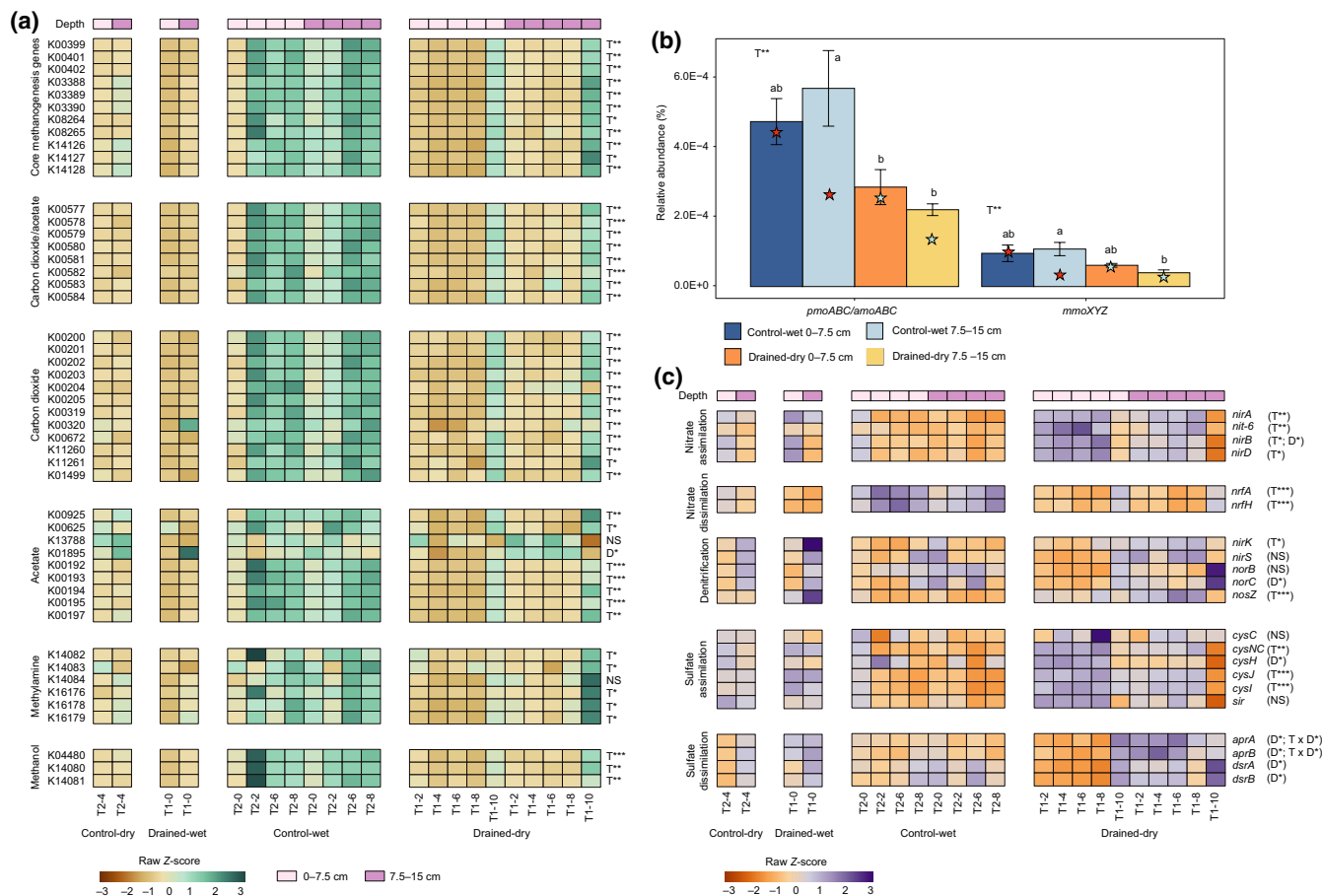
FIGURE 3 Shifts in microbial metabolisms in response to drainage. The relative abundance of (a) genes involved in methanogenesis from different pathways, including CO_2, acetate, methanol, and methylamines. The genes under the category "core methanogenesis genes" are used by all methanogens. (b) Relative abundance of genes encoding subunits of particulate methane/ammonia monooxygenase (*pmoABC/amoABC*) and soluble methane monooxygenase (*mmoXYZ*). Red and light blue star shapes on bar plot show data points of drained-wet and control-dry treatments, respectively. Different letters denote significant ($p < 0.05$) differences between groups. (c) Heatmaps depicting the relative abundances of genes involved in assimilatory and dissimilatory nitrate and sulfate reduction, and denitrification. *p*-values are indicated by asterisks **$p < 0.01$, ***$p < 0.001$ (two-way ANOVA)

distantly related to the cluster of *Ca.* "Methanoflorens stordalenmirensis" and *Ca.* "M. crilli" (Figure 4a). Two novel *Methanobacteriaceae* MAGs (Chersky.38_2 and Chersky.38_6) distantly related to known *Methanobacterium* genomes (<92.5% ANI; Figure 4b), accounted for 57.5%–62.9% of the total abundance of recovered archaeal MAGs in drained plots, but much less (23.3%–28.9%) in the control plots. Furthermore, two novel *Bathyarchaeota* MAGs were recovered from metagenome data, one (Chersky_322) belonging to the cluster B26-1 and the other (Chersky_747) to the cluster TCS64 (Figure 4d). They were less abundant (2.5%–12.7% of the total archaeal abundance) compared to the other methanogens but occurred consistently in both drained and control plots.

We compared the relative abundance of MAGs across all samples to identify the differentially abundant taxa between treatments (drained-dry vs. control-wet) and depth (surface vs. subsurface). In both surface and subsurface soils, huge reductions were observed in the abundance of all methanogen MAGs in the drained plots, compared to the control plots, except for one soil core (T1–10 in Figure

S8). Among the methanogen MAGs, *Methanoregula* revealed the most striking changes in abundance with treatment, which is in accordance with the aforementioned 16S rRNA gene- and *mcrA* gene-based results. To infer potential reasons for its drainage-induced abundance reduction, we performed enrichment analysis on functional genes (COG functions) across nine archaeal MAGs. The functional enrichment analysis revealed that the *Methanoregula* MAG lacks genes encoding small heat shock protein (HSP20 family) and DNA repair exonuclease SbcCD subunits ($p < 0.05$ and $q < 0.1$; Table S6).

Correlations between the relative abundances of MAGs coupled with metabolic reconstruction enabled the identification of novel metabolic interactions between methanogens and syntrophic taxa in CH_4 dynamics at this site. For example, strong positive correlations were observed between the relative abundances of *Methanobacteriaceae* and *Syntrophobacteraceae* MAGs (Figure 5a; $R^2 = 0.90$, $p < 0.0001$), and between *Methanoregula* and *Bathyarchaeota* MAGs (Figure 5b; $R^2 = 0.81$, $p < 0.0001$).

FIGURE 4 Phylogenetic reconstruction of archaeal metagenome-assembled genomes (MAGs). (a) *Methanomicrobia* subtree depicting *Methanoregulaceae*, *Methanosphaerulaceae*, and *Ca.* "Methanoflorentales" MAGs. (b) *Methanobacteriaceae* subtree incorporating *Methanobacteriaceae* MAGs. (c) *Methanosarcinaceae* subtree depicting *Methanosarcina* MAGs. (d) A subtree of *Bathyarchaeota* MAGs. Black and gray dots indicate bootstrap values ≥95% and ≥70%–95%, respectively. MAGs recovered in this study are colored in red. Recently reported *Ca.* "Methanoflorentales" MAGs in the Arctic were included in the *Methanomicrobia* subtree (in blue)

4 | DISCUSSION

4.1 | Drainage effects on microbial abundance, taxonomic composition, and CO_2 and CH_4 fluxes

In the present study, we demonstrated that long-term drainage has strongly influenced both the abundance and taxonomic composition of microbial communities. Low WT favoring aerobic microbial growth conditions in drained soils increased the fungal abundance, with results in accordance with those of other studies (Abdallah et al., 2019; Kwon et al., 2013). This may have partially contributed to an increase in R_h within the topsoil (0–15 cm) at the drained plots, as fungi decompose complex organic matter such as cellulose and lignin under aerobic conditions, promoting further decomposition and CO_2 emission (Sánchez, 2009; Wirsel, 2004). Our previous incubation experiment showed that R_h was 82% higher within the surface soil of drained-dry plots compared to that of control-wet under the same temperature regimes (Kwon et al., 2019). This finding supports the tight correlation between increased fungal abundance and CO_2 emission. In addition to the increased fungal abundance, warmer

surface soil temperatures at the drained plots (data shown, e.g., in Kwon et al., 2019; Göckede et al., 2019) may have further accelerated microbial respiration/activity (Bradford, 2013; Frey et al., 2013; Karhu et al., 2014). Unlike CH_4, it is challenging to track the functional genes or groups that produce CO_2 and associate them with CO_2 emissions, as most of the microbes respire and thus contribute to CO_2 emissions.

Soil bacterial communities responded strongly to drainage. Some bacterial taxa such as *Bacteroidetes* (particularly order *Bacteroidales*) and *Chloroflexi* (*Anaerolinaeles*) were more susceptible to drainage, whereas others such as *Acidobacteria* (*Solibacterales*), *Alphaproteobacteria* (*Rhizobiales*), and *Betaproteobacteria* (*Burkholderiales*) were more abundant under dry conditions. Similar results were observed in previous studies comparing the microbial communities between inundated and upland tundra soils (Shi et al., 2015; Taş et al., 2018; Woodcroft et al., 2018). Long-term, drainage-induced changes in ecosystem properties—particularly biogeochemical conditions and plant community structure that have been demonstrated in our previous studies (Kwon et al., 2016, 2017)—may have contributed to the increase or decrease in the relative
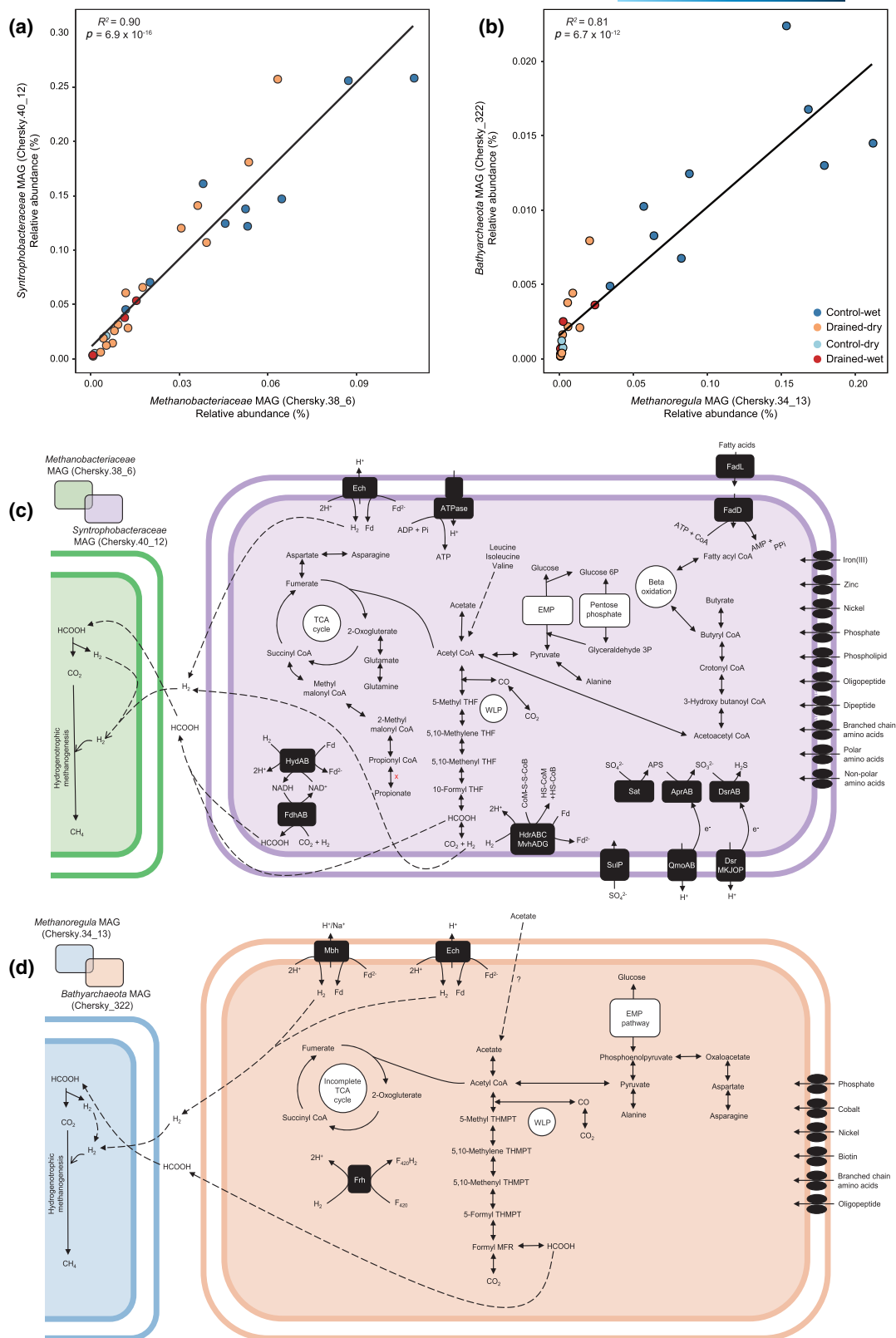
FIGURE 5 Novel syntrophic relationships in methanogenesis. (a) Correlation of the relative abundances of *Methanobacteriaceae* and *Syntrophobacteraceae* MAGs. (b) Correlation of the relative abundances of *Methanoregula* and *Bathyarchaeota* MAGs. Metabolic reconstruction of (c) *Syntrophobacteraceae* and (d) *Bathyarchaeota* MAGs. Dotted lines indicate enzyme-independent hydrogen movement. Green and blue cell cartoons depict *Methanobacteriaceae* and *Methanoregula* MAGs, respectively, consuming hydrogen produced by *Syntrophobacteraceae* and *Bathyarchaeota* MAGs

abundance of these microbial taxa. A key feature of the shifts within the archaeal community was the disappearance of *Methanoregula* following drainage. Members of *Methanoregula* are hydrogenotrophic methanogens (Bräuer et al., 2011; Yashiro et al., 2011) and their growth is inhibited even under trace quantities of oxygen (Yashiro et al., 2011); hence, they are less likely to inhabit oxygenated drained soils. Moreover, given that small heat shock proteins and DNA repair systems are known to be involved in oxidative stress tolerance, the absence of those genes in the *Methanoregula* MAG may be responsible for its low tolerance to drainage-induced oxidative stress (Ma et al., 2021; Singh et al., 2014). These factors may have largely contributed to a substantial decrease in CH_4 emissions at the drained site (McCalley et al., 2014; Yang et al., 2017).

Drained-dry showed similar microbial communities, functional gene abundances, and Rh and CH_4 fluxes to those of control-dry, whereas drained-wet showed characteristics between those of control-wet and drained-dry. It implies that artificial drainage manipulation shifted the characteristics of wet Arctic floodplain toward those of naturally dry micro-site, that is, hummocks. Yet, drained-dry showed different vegetation community composition from control-dry (Kwon et al., 2016), and further observations would be needed if this modification toward control-dry during the last decade would continue, stop, or change a direction.

4.2 | Drainage effects on microbial metabolism related to CH_4 and CH_4 fluxes

Consistent with the taxonomic community composition, the functional genes revealed strong shifts in composition following drainage, particularly genes involved in the CH_4 metabolism. The relative abundance of genes involved in both methanogenesis and methanotrophy was decreased following drainage, and the considerably reduced abundance of methanogens may be a crucial driving force for the significantly reduced CH_4 flux at the drained plots. Methanogenesis is favored in wet soils because they contain low amounts of dissolved O_2. Moreover, the concentrations of organic acids and fermentation products such as H_2 and CO_2 could have increased in wet soils due to the higher proportion of functional genes involved in the metabolism of simple carbohydrates and fermentation (Figure S4), which may have further fueled CH_4 production in the control plots.

Anoxic conditions in control plots boosted methanogenesis, and the elevated CH_4 concentration and locally available O_2 at plant roots (Perryman et al., 2020; Wolf et al., 2007) may have maintained a higher proportion of methanotrophic populations than that at the drained plots, which can oxidize up to 90% of the produced CH_4 in the rhizosphere (Holzapfel-Pschorn et al., 1985; Oremland & Culbertson, 1992). Among the methanotrophic lineages, the abundance reduction in the drained plots was pronounced in the *Methylococcales* taxa encoding particulate methane monooxygenase. This is in accordance with a recent finding in a naturally thawing permafrost environment: both *Methylococcaceae pmoA* genes and transcripts were prevalent

in the fully thawed fen, where the WT is often located above the peat surface, but not in bog or palsa environments, where WT is below the peat surface (Singleton et al., 2018). These findings, that is, the greater abundance of *Methylobacter* sp. in control plots), are also consistent with the results of our previous study, which was conducted at the same site as this study (Kwon et al., 2017). This collectively suggests that *Methylococcales* are crucial in CH_4 oxidation and, thus for net CH_4 emissions, under the microaerobic conditions in inundated environments in the Arctic. A high CH_4 production potential (microbial potential for CH_4 production, inferred from gene abundances) was observed in some surface and subsurface soils of the drained-dry plot (T1–10 in Figure 3a; Figure S8), yet significantly lower CH_4 emission rates compared to control-wet plot (Kwon et al., 2017) imply that a substantial amount of CH_4 was oxidized. Additionally, higher aerenchymatous plant (*E. angustifolium*) density at this sampling point (T1-10) suggests that the WT might be marginally influenced by drainage, as *E. angustifolium* was shown to dominate in control-wet soils (Kwon et al., 2016, 2017). The high-affinity methanotroph clade USCα had the greatest abundance in control-wet soils, and were also predominant in drained-dry soils, which suggests that their growth is not just regulated by CH_4 concentrations, but they can also adapt to facultative methanotrophic lifestyle to survive on other substrates such as acetate or other atmospheric trace gases such as CO and H_2 (Semrau et al., 2011; Singleton et al., 2018). Recent findings suggested that traditional clades known for low-affinity methanotrophs can also oxidize atmospheric methane (Cai et al., 2016; Kravchenko et al., 2010; Tveit et al., 2019). Given that the relative abundance of *Methylocystaceae mmoX* is higher in the surface soils than in the subsurface soils at both treatment sites, and members of several methanotrophic genera belonging to this family are known to consume atmospheric methane (Cai et al., 2016; Tveit et al., 2019), they may also play a role in atmospheric methane oxidation together with USCα clade in this environment.

4.3 | Drainage effects on anaerobic microbial metabolism

Drier soil conditions following decade-long drainage led to an increase in the abundances of oxygen-specific respiratory metabolisms, such as cytochrome *c* oxidase genes (Figure S7), and further led to a decline in the relative abundances of genes involved in anaerobic metabolic processes, for example, methanogenesis and dissimilatory nitrate reduction to ammonium (DNRA). A decrease in nitrite but an increase in nitrate concentrations in drained plots may imply enhanced nitrification and/or suppressed denitrification under oxic conditions. Partial denitrification is possible at subsurface layers (under less oxic conditions), given that nitrite concentration was reduced while some denitrification-related genes (*nirK* and *nosZ*) in subsurface soils were increased. The control-wet soils with relatively lower N concentration could have also promoted the enrichment of DNRA genes (*nrfA* and *nrfH*), which can greatly contribute to soil N retention. In contrast to our expectations, higher dissimilatory

sulfate reduction potential as well as significant ($p < 0.05$) reduction in sulfate concentrations were observed in subsurface soils following drainage, which experience fluctuating oxic and anoxic conditions. Sulfate-reducing microorganisms can outcompete methanogens for hydrogen and acetate (Lovley & Klug, 1983); however, presumably, relatively low concentrations of sulfate, a typical characteristic of Arctic tundra soils (Newman et al., 2015), did not favor sulfate reduction in control soils dominated by methanogens. The higher nitrate and sulfate concentrations in drained soils could have increased the relative dominance of genes associated with assimilatory nitrate and sulfate reduction.

4.4 | Novel methanogenic archaea and syntrophy in methanogenesis

Metagenome assembly and binning led to the recovery of several novel methanogen MAGs. A draft genome of a *Ca.* "Methanoflorentales" lineage, evolutionarily distant from the *Ca.* "Methanoflorens" group, was assembled and the MAG abundance result revealed that this lineage is one of the abundant methanogens in the deeper layer of the Siberian floodplain. Previous studies reported that members of *Ca.* "Methanoflorens" sp. are widespread across the Arctic permafrost regions (Mondav et al., 2014; Woodcroft et al., 2018). The reconstructed genome phylogeny revealed that this novel lineage formed a monophyletic cluster with those obtained from the tundra soils of Alaska and Northern Sweden at the species level (97.8%–99.7% ANI), suggesting that this hydrogenotrophic methanogen may also occur widely across the circum-Arctic region.

The *Methanosarcina* MAG (Chersky.40_19) was also one of the abundant methanogenic lineages in wet conditions. Members of *Methanosarcina* spp. are among the most frequently occurring methanogens in permafrost environments, but information on their metabolic capabilities and physiology is very limited because only a few strains (*M. mazei* JL01, *M. soligelidi* SMA-21, and *Methanosarcina* sp. SMA-17) have been isolated from Arctic permafrost habitats (Serrano et al., 2019; Vishnivetskaya et al., 2018; Wagner & Liebner, 2010). This MAG was distantly related to genomes of other Methanosarcina lineages, suggesting that either this lineage may not be widespread in the polar habitats or it may be simply due to the lack of permafrost-derived genomes available. Interestingly, this MAG was most closely matched with *Methanosarcina* sp. Ant1 MAG (96.2% ANI; Figure 4c), which was found in the 15,000-year-old permafrost of the Antarctic Dry Valley (Vishnivetskaya et al., 2018). Regarding the high methanogenic activity of Ant1 at 20°C, but not at 6°C, in a decadal microcosm, the sister clade (Chersky.40_19) might also have the potential to produce more methane in response to future warming in the Siberian Arctic.

The metabolic reconstruction of the *Syntrophobacteraceae* MAG revealed the presence of genes involved in sulfate reduction; acetate, butyrate, and propionate oxidation; and proton/hydrogen interconversion, suggesting that members of this lineage can grow under facultative syntrophic association. *Syntrophobacteraceae* have been identified as one of the major sulfate-reducing bacteria and have been reported to play important roles in the oxidation of short-chain fatty acids, such as acetate, butyrate, and propionate (Liu & Conrad, 2017; Liu et al., 2018). The strong correlation between the relative abundances of *Syntrophobacteraceae* and *Methanobacteriaceae* MAGs indicates that these lineages are possibly in a syntrophic relationship through intermediate (formate or hydrogen)-dependent interspecies electron transfer. The hydrogenotrophic methanogens (here *Methanobacteriaceae*) presumably maintain a low hydrogen partial pressure that allows the oxidation of organic compounds more favorable for syntrophs (here *Syntrophobacteraceae*; Stams & Plugge, 2009). Furthermore, a strong correlation observed between the relative abundances of *Bathyarchaeota* and *Methanoregula* MAGs suggests the possibility of a syntrophic association between these two lineages. The *Bathyarchaeota* MAG has acetyl-CoA synthetase (Acd) for acetate production or assimilation, and recent genomic and functional analyses have revealed that some members of *Bathyarchaeota* are acetogenic (He et al., 2016). Hence, these two lineages could be in a syntrophic relationship for methane production by syntrophic acetate oxidation. The possible syntrophic association of *Bathyarchaeota* with members of *Methanomicrobia*, including *Methanoregula*, was also suggested in earlier studies through their frequent co-occurrence (Xiang et al., 2017) and close physical association (Collins et al., 2005).

5 | CONCLUSIONS

This study demonstrates that a decade of drainage manipulation led to significant changes in the abundance, taxonomy, and functions of soil microbial communities in the Arctic wetland. Drainage effects are particularly pronounced in the abundance and composition of microbial taxa associated with methane production and oxidation. Drainage markedly reduced the abundance of both methanogens and methanotrophs, which well parallels the highly reduced CH_4 emissions. Certain microbial lineages were more susceptible to the dried condition compared to other lineages, with the abundance of *Methanoregula* and *Methylococcales* being markedly decreased in response to drainage. The analysis of recovered MAGs and their metabolism demonstrated that CH_4 is mostly generated by several novel methanogens, and syntrophy may play an important role in methanogenesis at this site. These results enabled a deeper mechanistic understanding of relationships between microbial processes and GHG dynamics. Genes and genomic information of novel microbial lineages, responding differentially to the drainage, will facilitate the development of suitable diagnostic biomarkers (e.g., genes of drying-sensitive microbial taxa) which can help to improve descriptions of microbial processes in global biogeochemical models. Furthermore, the identification of novel syntrophic relationships between methanogens and syntrophic partners, and their reconstructed metabolic pathways will further facilitate the targeted culturing of as-yet-cultivated methanogens and the characterization of their ecological roles in the Arctic wetland ecosystems.

AUTHOR CONTRIBUTION

Min Jung Kwon, Binu M. Tripathi, and Mincheol Kim conceived the study, and Mathias Göckede designed the experiment and maintained the experimental site; Min Jung Kwon collected soil samples, measured soil chemical properties and CO_2 and CH_4 fluxes, and performed DNA extraction; Min Jung Kwon and Nu Ri Myeong prepared samples for DNA sequencing; Binu M. Tripathi performed qPCR assays; Min Jung Kwon, Binu M. Tripathi, Mincheol Kim, and Seung Chul Shin performed data analysis; Min Jung Kwon, Binu M. Tripathi, and Mincheol Kim wrote the manuscript with feedbacks from all authors.

DATA AVAILABILITY STATEMENT

All sequences including metagenome and amplicon sequence data have been submitted to the NCBI Sequence Read Archive (SRA) database under the BioProject accession number PRJNA588342. Sequences of MAGs were deposited to the SRA under accession numbers provided in Table S5. Chamber flux data used in this study are available here (https://edmond.mpdl.mpg.de/imeji/collection/s_7fISn_9tbU11WM).

ORCID

Min Jung Kwon https://orcid.org/0000-0002-7330-2320
Binu M. Tripathi https://orcid.org/0000-0002-7848-0206
Mathias Göckede https://orcid.org/0000-0003-2833-8401
Seung Chul Shin https://orcid.org/0000-0001-6835-484X
Nu Ri Myeong https://orcid.org/0000-0002-6390-5339
Yoo Kyung Lee https://orcid.org/0000-0002-1271-5738
Mincheol Kim https://orcid.org/0000-0003-1506-4800

REFERENCES

Aas, K. S., Martin, L., Nitzbon, J., Langer, M., Boike, J., Lee, H., Berntsen, T. K., & Westermann, S. (2019). Thaw processes in ice-rich permafrost landscapes represented with laterally coupled tiles in a land surface model. *The Cryosphere*, *13*(2), 591–609. https://doi.org/10.5194/tc-13-591-2019

Abdallah, R. Z., Wegner, C.-E., & Liesack, W. (2019). Community transcriptomics reveals drainage effects on paddy soil microbiome across all three domains of life. *Soil Biology and Biochemistry*, *132*, 131–142. https://doi.org/10.1016/j.soilbio.2019.01.023

Avis, C. A., Weaver, A. J., & Meissner, K. J. (2011). Reduction in areal extent of high-latitude wetlands in response to permafrost thaw. *Nature Geoscience*, *4*, 444–448. https://doi.org/10.1038/ngeo1160

Bolger, A. M., Lohse, M., & Usadel, B. (2014). Trimmomatic: A flexible trimmer for Illumina sequence data. *Bioinformatics*, *30*(15), 2114–2120. https://doi.org/10.1093/bioinformatics/btu170

Bond-Lamberty, B., & Thomson, A. (2010). Temperature-associated increases in the global soil respiration record. *Nature*, *464*(7288), 579–582. https://doi.org/10.1038/nature08930

Boyd, J. A., Woodcroft, B. J., & Tyson, G. W. (2018). GraftM: A tool for scalable, phylogenetically informed classification of genes within metagenomes. *Nucleic Acids Research*, *46*(10), e59. https://doi.org/10.1093/nar/gky174

Bradford, M. A. (2013). Thermal adaptation of decomposer communities in warming soils. *Frontiers in Microbiology*, *4*. https://doi.org/10.3389/fmicb.2013.00333

Bräuer, S. L., Cadillo-Quiroz, H., Ward, R. J., Yavitt, J. B., & Zinder, S. H. (2011). *Methanoregula boonei* gen. Nov., sp. Nov., an acidiphilic methanogen isolated from an acidic peat bog. *International Journal of Systematic and Evolutionary Microbiology*, *61*(Pt 1), 45–52. https://doi.org/10.1099/ijs.0.021782-0

Buchfink, B., Xie, C., & Huson, D. H. (2015). Fast and sensitive protein alignment using DIAMOND. *Nature Methods*, *12*(1), 59–60. https://doi.org/10.1038/nmeth.3176

Cai, Y., Zheng, Y., Bodelier, P. L. E., Conrad, R., & Jia, Z. (2016). Conventional methanotrophs are responsible for atmospheric methane oxidation in paddy soils. *Nature Communications*, *7*, 11728. https://doi.org/10.1038/ncomms11728

Collins, G., O'Connor, L., Mahony, T., Gieseke, A., de Beer, D., & O'Flaherty, V. (2005). Distribution, localization, and phylogeny of abundant populations of Crenarchaeota in anaerobic granular sludge. *Applied and Environmental Microbiology*, *71*(11), 7523–7527. https://doi.org/10.1128/AEM.71.11.7523-7527.2005

Comeau, A. M., Douglas, G. M., & Langille, M. G. I. (2017). Microbiome helper: A custom and streamlined workflow for microbiome research. *mSystems*, *2*(1). https://doi.org/10.1128/mSystems.00127-16

Davidson, E. A., & Janssens, I. A. (2006). Temperature sensitivity of soil carbon decomposition and feedbacks to climate change. *Nature*, *440*(7081), 165–173. https://doi.org/10.1038/nature04514

Farquharson, L. M., Romanovsky, V. E., Cable, W. L., Walker, D. A., Kokelj, S. V., & Nicolsky, D. (2019). Climate change drives widespread and rapid thermokarst development in very cold permafrost in the Canadian High Arctic. *Geophysical Research Letters*, *46*(12), 6681–6689. https://doi.org/10.1029/2019GL082187

Frey, S. D., Lee, J., Melillo, J. M., & Six, J. (2013). The temperature response of soil microbial efficiency and its feedback to climate. *Nature Climate Change*, *3*(4), 395–398. https://doi.org/10.1038/nclimate1796

Göckede, M., Kittler, F., Kwon, M. J., Burjack, I., Heimann, M., Kolle, O., Zimov, N., & Zimov, S. (2017). Shifted energy fluxes, increased Bowen ratios, and reduced thaw depths linked with drainage-induced changes in permafrost ecosystem structure. *The Cryosphere*, *11*(6), 2975–2996. https://doi.org/10.5194/tc-11-2975-2017

Göckede, M., Kwon, M. J., Kittler, F., Heimann, M., Zimov, N., & Zimov, S. (2019). Negative feedback processes following drainage slow down permafrost degradation. *Global Change Biology*, *25*(10), 3254–3266. https://doi.org/10.1111/gcb.14744

He, Y., Li, M., Perumal, V., Feng, X., Fang, J., Xie, J., Sievert, S. M., & Wang, F. (2016). Genomic and enzymatic evidence for acetogenesis among multiple lineages of the archaeal phylum Bathyarchaeota widespread in marine sediments. *Nature Microbiology*, *1*(6), 16035. https://doi.org/10.1038/nmicrobiol.2016.35

Hicks Pries, C. E., Schuur, E. A. G., Natali, S. M., & Crummer, K. G. (2016). Old soil carbon losses increase with ecosystem respiration in

experimentally thawed tundra. *Nature Climate Change*, 6, 214–218. https://doi.org/10.1038/nclimate2830

Holzapfel-Pschorn, A., Conrad, R., & Seiler, W. (1985). Production, oxidation and emission of methane in rice paddies. *FEMS Microbiology Letters*, 31(6), 343–351. https://doi.org/10.1016/0378-1097(85)90030-8

Huang, J., Zhang, X., Zhang, Q., Lin, Y., Hao, M., Luo, Y., Zhao, Z., Yao, Y., Chen, X., Wang, L., Nie, S., Yin, Y., Xu, Y., & Zhang, J. (2017). Recently amplified arctic warming has contributed to a continual global warming trend. *Nature Climate Change*, 7, 875–879. https://doi.org/10.1038/s41558-017-0009-5

Huson, D. H., Auch, A. F., Qi, J., & Schuster, S. C. (2007). MEGAN analysis of metagenomic data. *Genome Research*, 17(3), 377–386. https://doi.org/10.1101/gr.5969107

Johnston, C. E., Ewing, S. A., Harden, J. W., Varner, R. K., Wickland, K. P., Koch, J. C., Fuller, C. C., Manies, K., & Jorgenson, M. T. (2014). Effect of permafrost thaw on CO_2 and CH_4 exchange in a western Alaska peatland chronosequence. *Environmental Research Letters*, 9(8), 085004. https://doi.org/10.1088/1748-9326/9/8/085004

Karhu, K., Auffret, M. D., Dungait, J. A. J., Hopkins, D. W., Prosser, J. I., Singh, B. K., Subke, J.-A., Wookey, P. A., Agren, G. I., Sebastià, M.-T., Gouriveau, F., Bergkvist, G., Meir, P., Nottingham, A. T., Salinas, N., & Hartley, I. P. (2014). Temperature sensitivity of soil respiration rates enhanced by microbial community response. *Nature*, 513(7516), 81–84. https://doi.org/10.1038/nature13604

Kittler, F., Heimann, M., Kolle, O., Zimov, N., Zimov, S., & Göckede, M. (2017). Long-term drainage reduces CO_2 uptake and CH_4 emissions in a Siberian permafrost ecosystem. *Global Biogeochemical Cycles*, 31(12), 1704–1717. https://doi.org/10.1002/2017GB005774

Kopylova, E., Noé, L., & Touzet, H. (2012). SortMeRNA: Fast and accurate filtering of ribosomal RNAs in metatranscriptomic data. *Bioinformatics*, 28(24), 3211–3217. https://doi.org/10.1093/bioinformatics/bts611

Kravchenko, I. K., Kizilova, A. K., Bykova, S. A., Men'ko, E. V., & Gal'chenko, V. F. (2010). Molecular analysis of high-affinity methane-oxidizing enrichment cultures isolated from a forest biocenosis and agrocenoses. *Microbiology*, 79(1), 106–114. https://doi.org/10.1134/S0026261710010145

Kwon, M. J., Beulig, F., Ille, I., Wildner, M., Küsel, K., Merbold, L., Mahecha, M., Zimov, N., Zimov, S. A., Heimann, M., Schuur, E. A. G., Kostka, J., Kolle, O., Hilke, I., & Göckede, M. (2017). Plants, microorganisms and soil temperatures contribute to a decrease in methane fluxes on a drained Arctic floodplain. *Global Change Biology*, 23(6), 2396–2412. https://doi.org/10.1111/gcb.13558

Kwon, M. J., Haraguchi, A., & Kang, H. (2013). Long-term water regime differentiates changes in decomposition and microbial properties in tropical peat soils exposed to the short-term drought. *Soil Biology and Biochemistry*, 60, 33–44. https://doi.org/10.1016/j.soilbio.2013.01.023

Kwon, M. J., Heimann, M., Kolle, O., Luus, K. A., Schuur, E. A. G., Zimov, N., Zimov, S. A., & Göckede, M. (2016). Long-term drainage reduces CO_2 uptake and increases CO_2 emission on a Siberian floodplain due to shifts in vegetation community and soil thermal characteristics. *Biogeosciences*, 13, 4219–4235. https://doi.org/10.5194/bg-13-4219-2016

Kwon, M. J., Natali, S. M., Hicks Pries, C. E., Schuur, E. A. G., Steinhof, A., Crummer, K. G., Zimov, N., Zimov, S. A., Heimann, M., Kolle, O., & Göckede, M. (2019). Drainage enhances modern soil carbon contribution but reduces old soil carbon contribution to ecosystem respiration in tundra ecosystems. *Global Change Biology*, 25(4), 1315–1325. https://doi.org/10.1111/gcb.14578

Lawrence, D. M., Koven, C. D., Swenson, S. C., Riley, W. J., & Slater, A. G. (2015). Permafrost thaw and resulting soil moisture changes regulate projected high-latitude CO_2 and CH_4 emissions. *Environmental Research Letters*, 10(9), 094011. https://doi.org/10.1088/1748-9326/10/9/094011

Liljedahl, A. K., Boike, J., Daanen, R. P., Fedorov, A. N., Frost, G. V., Grosse, G., Hinzman, L. D., Iijma, Y., Jorgenson, J. C., Matveyeva, N., Necsoiu, M., Raynolds, M. K., Romanovsky, V. E., Schulla, J., Tape, K. D., Walker, D. A., Wilson, C. J., Yabuki, H., & Zona, D. (2016). Pan-Arctic ice-wedge degradation in warming permafrost and its influence on tundra hydrology. *Nature Geoscience*, 9, 312–318. https://doi.org/10.1038/ngeo2674

Liu, P., & Conrad, R. (2017). Syntrophobacteraceae-affiliated species are major propionate-degrading sulfate reducers in paddy soil. *Environmental Microbiology*, 19(4), 1669–1686. https://doi.org/10.1111/1462-2920.13698

Liu, P., Pommerenke, B., & Conrad, R. (2018). Identification of Syntrophobacteraceae as major acetate-degrading sulfate reducing bacteria in Italian paddy soil. *Environmental Microbiology*, 20(1), 337–354. https://doi.org/10.1111/1462-2920.14001

Lovley, D. R., & Klug, M. J. (1983). Sulfate reducers can outcompete methanogens at freshwater sulfate concentrations. *Applied and Environmental Microbiology*, 45(1), 187–192. https://doi.org/10.1128/aem.45.1.187-192.1983

Ma, P., Li, J., Qi, L., & Dong, X. (2021). The archaeal small heat shock protein Hsp17.6 protects proteins from oxidative inactivation. *International Journal of Molecular Sciences*, 22(5), 2591. https://doi.org/10.3390/ijms22052591

McCalley, C. K., Woodcroft, B. J., Hodgkins, S. B., Wehr, R. A., Kim, E.-H., Mondav, R., Crill, P. M., Chanton, J. P., Rich, V. I., Tyson, G. W., & Saleska, S. R. (2014). Methane dynamics regulated by microbial community response to permafrost thaw. *Nature*, 514(7523), 478–481. https://doi.org/10.1038/nature13798

Mondav, R., Woodcroft, B. J., Kim, E.-H., McCalley, C. K., Hodgkins, S. B., Crill, P. M., Chanton, J., Hurst, G. B., VerBerkmoes, N. C., Saleska, S. R., Hugenholtz, P., Rich, V. I., & Tyson, G. W. (2014). Discovery of a novel methanogen prevalent in thawing permafrost. *Nature Communications*, 5, 3212. https://doi.org/10.1038/ncomms4212

Newman, B. D., Throckmorton, H. M., Graham, D. E., Gu, B., Hubbard, S. S., Liang, L., Wu, Y., Heikoop, J. M., Herndon, E. M., Phelps, T. J., Wilson, C. J., & Wullschleger, S. D. (2015). Microtopographic and depth controls on active layer chemistry in Arctic polygonal ground. *Geophysical Research Letters*, 42(6), 1808–1817. https://doi.org/10.1002/2014GL062804

Olefeldt, D., Goswami, S., Grosse, G., Hayes, D., Hugelius, G., Kuhry, P., McGuire, A. D., Romanovsky, V. E., Sannel, A. B. K., Schuur, E. A. G., & Turetsky, M. R. (2016). Circumpolar distribution and carbon storage of thermokarst landscapes. *Nature Communications*, 7(1), 13043. https://doi.org/10.1038/ncomms13043

Oremland, R. S., & Culbertson, C. W. (1992). Importance of methane-oxidizing bacteria in the methane budget as revealed by the use of a specific inhibitor. *Nature*, 356, 421–423. https://doi.org/10.1038/356421a0

Osterkamp, T. E., Jorgenson, M. T., Schuur, E. A. G., Shur, Y. L., Kanevskiy, M. Z., Vogel, J. G., & Tumskoy, V. E. (2009). Physical and ecological changes associated with warming permafrost and thermokarst in Interior Alaska. *Permafrost and Periglacial Processes*, 20(3), 235–256. https://doi.org/10.1002/ppp.656

Perryman, C. R., McCalley, C. K., Malhotra, A., Fahnestock, M. F., Kashi, N. N., Bryce, J. G., Giesler, R., & Varner, R. K. (2020). Thaw transitions and redox conditions drive methane oxidation in a permafrost peatland. *Journal of Geophysical Research: Biogeosciences*, 125(3), e2019JG005526. https://doi.org/10.1029/2019JG005526

R Development Core Team. (2013). *R: A language and environment for statistical computing*. R Foundation for Statistical Computing. http://www.r-project.org

Rodenhizer, H., Ledman, J., Mauritz, M., Natali, S. M., Pegoraro, E., Plaza, C., Romano, E., Schädel, C., Taylor, M., & Schuur, E. (2020). Carbon thaw rate doubles when accounting for subsidence in a permafrost warming experiment. *Journal of Geophysical Research: Biogeosciences*, 125(6), e2019JG005528. https://doi.org/10.1029/2019JG005528

Rodriguez-R, L. M., Gunturu, S., Tiedje, J. M., Cole, J. R., & Konstantinidis, K. T. (2018). Nonpareil 3: Fast estimation of metagenomic coverage and sequence diversity. *mSystems*, *3*(3). https://doi.org/10.1128/mSystems.00039-18

Salehi, Z., & Najafi, M. (2014). RNA preservation and stabilization. *Biochemistry & Physiology: Open Access*, *3*(126). https://doi.org/10.4172/2168-9652.1000126

Sánchez, C. (2009). Lignocellulosic residues: Biodegradation and bioconversion by fungi. *Biotechnology Advances*, *27*(2), 185–194. https://doi.org/10.1016/j.biotechadv.2008.11.001

Schädel, C., Bader, M.-F., Schuur, E. A. G., Biasi, C., Bracho, R., Čapek, P., De Baets, S., Diáková, K., Ernakovich, J., Estop-Aragones, C., Graham, D. E., Hartley, I. P., Iversen, C. M., Kane, E., Knoblauch, C., Lupascu, M., Martikainen, P. J., Natali, S. M., Norby, R. J., … Wickland, K. P. (2016). Potential carbon emissions dominated by carbon dioxide from thawed permafrost soils. *Nature Climate Change*, *6*(10), 950–953. https://doi.org/10.1038/nclimate3054

Schirrmeister, L., Froese, D., Tumskoy, V., Grosse, G., & Wetterich, S. (2013). Yedoma: Late Pleistocene ice-rich syngenetic permafrost of Beringia. In *Encyclopedia of quaternary science* (pp. 542–552). Elsevier. https://doi.org/10.1016/B978-0-444-53643-3.00106-0

Schirrmeister, L., Siegert, C., Kuznetsova, T., Kuzmina, S., Andreev, A., Kienast, F., Meyer, H., & Bobrov, A. (2002). Paleoenvironmental and paleoclimatic records from permafrost deposits in the Arctic region of Northern Siberia. *Quaternary International*, *89*(1), 97–118. https://doi.org/10.1016/S1040-6182(01)00083-0

Schloss, P. D. P., Westcott, S. S. L., Ryabin, T., Hall, J. R. J., Hartmann, M., Hollister, E. B. E., Lesniewski, R. R. A., Oakley, B. B., Parks, D. H. D., Robinson, C. C. J., Sahl, J. J. W., Stres, B., Thallinger, G. G. G., Van Horn, D. D. J., & Weber, C. F. C. (2009). Introducing mothur: Open-source, platform-independent, community-supported software for describing and comparing microbial communities. *Applied and Environmental Microbiology*, *75*(23), 7537–7541. https://doi.org/10.1128/AEM.01541-09

Schuur, E. A. G., McGuire, A. D., Schädel, C., Grosse, G., Harden, J. W., Hayes, D. J., Hugelius, G., Koven, C. D., Kuhry, P., Lawrence, D. M., Natali, S. M., Olefeldt, D., Romanovsky, V. E., Schaefer, K., Turetsky, M. R., Treat, C. C., & Vonk, J. E. (2015). Climate change and the permafrost carbon feedback. *Nature*, *520*, 171–179. https://doi.org/10.1038/nature14338

Schuur, E. A. G., Vogel, J. G., Crummer, K. G., Lee, H., Sickman, J. O., & Osterkamp, T. E. (2009). The effect of permafrost thaw on old carbon release and net carbon exchange from tundra. *Nature*, *459*, 556–559. https://doi.org/10.1038/nature08031

Semrau, J. D., DiSpirito, A. A., & Vuilleumier, S. (2011). Facultative methanotrophy: False leads, true results, and suggestions for future research. *FEMS Microbiology Letters*, *323*(1), 1–12. https://doi.org/10.1111/j.1574-6968.2011.02315.x

Serrano, P., Alawi, M., de Vera, J.-P., & Wagner, D. (2019). Response of methanogenic archaea from Siberian permafrost and non-permafrost environments to simulated mars-like desiccation and the presence of perchlorate. *Astrobiology*, *19*(2), 197–208. https://doi.org/10.1089/ast.2018.1877

Serreze, M. C., & Barry, R. G. (2011). Processes and impacts of Arctic amplification: A research synthesis. *Global and Planetary Change*, *77*(1–2), 85–96. https://doi.org/10.1016/j.gloplacha.2011.03.004

Shaiber, A., Willis, A. D., Delmont, T. O., Roux, S., Chen, L.-X., Schmid, A. C., Yousef, M., Watson, A. R., Lolans, K., Esen, Ö. C., Lee, S. T. M., Downey, N., Morrison, H. G., Dewhirst, F. E., Mark Welch, J. L., & Eren, A. M. (2020). Functional and genetic markers of niche partitioning among enigmatic members of the human oral microbiome. *Genome Biology*, *21*(1), 292. https://doi.org/10.1186/s13059-020-02195-w

Shi, Y., Xiang, X., Shen, C., Chu, H., Neufeld, J. D., Walker, V. K., & Grogan, P. (2015). Vegetation-associated impacts on Arctic tundra bacterial and microeukaryotic communities. *Applied and Environmental Microbiology*, *81*(2), 492–501. https://doi.org/10.1128/AEM.03229-14

Singh, H., Appukuttan, D., & Lim, S. (2014). Hsp20, a small heat shock protein of *Deinococcus radiodurans*, confers tolerance to hydrogen peroxide in *Escherichia coli*. *Journal of Microbiology and Biotechnology*, *24*(8), 1118–1122. https://doi.org/10.4014/jmb.1403.03006

Singleton, C. M., McCalley, C. K., Woodcroft, B. J., Boyd, J. A., Evans, P. N., Hodgkins, S. B., Chanton, J. P., Frolking, S., Crill, P. M., Saleska, S. R., Rich, V. I., & Tyson, G. W. (2018). Methanotrophy across a natural permafrost thaw environment. *The ISME Journal*, *12*, 2544–2558. https://doi.org/10.1038/s41396-018-0065-5

Stams, A. J. M., & Plugge, C. M. (2009). Electron transfer in syntrophic communities of anaerobic bacteria and archaea. *Nature Reviews Microbiology*, *7*(8), 568–577. https://doi.org/10.1038/nrmicro2166

Stewart, R. D., Auffret, M. D., Warr, A., Wiser, A. H., Press, M. O., Langford, K. W., Liachko, I., Snelling, T. J., Dewhurst, R. J., Walker, A. W., Roehe, R., & Watson, M. (2018). Assembly of 913 microbial genomes from metagenomic sequencing of the cow rumen. *Nature Communications*, *9*(1), 870. https://doi.org/10.1038/s41467-018-03317-6

Strauss, J., Schirrmeister, L., Grosse, G., Fortier, D., Hugelius, G., Knoblauch, C., Romanovsky, V., Schädel, C., Schneider von Deimling, T., Schuur, E. A. G., Shmelev, D., Ulrich, M., & Veremeeva, A. (2017). Deep Yedoma permafrost: A synthesis of depositional characteristics and carbon vulnerability. *Earth-Science Reviews*, *172*, 75–86. https://doi.org/10.1016/J.EARSCIREV.2017.07.007

Taş, N., Prestat, E., Wang, S., Wu, Y., Ulrich, C., Kneafsey, T., Tringe, S. G., Torn, M. S., Hubbard, S. S., & Jansson, J. K. (2018). Landscape topography structures the soil microbiome in arctic polygonal tundra. *Nature Communications*, *9*, 777. https://doi.org/10.1038/s41467-018-03089-z

Tveit, A. T., Hestnes, A. G., Robinson, S. L., Schintlmeister, A., Dedysh, S. N., Jehmlich, N., von Bergen, M., Herbold, C., Wagner, M., Richter, A., & Svenning, M. M. (2019). Widespread soil bacterium that oxidizes atmospheric methane. *Proceedings of the National Academy of Sciences of the United States of America*, *116*(17), 8515–8524. https://doi.org/10.1073/pnas.1817812116

van der Kolk, H. J., Heijmans, M. M. P. D., van Huissteden, J., Pullens, J. W. M., & Berendse, F. (2016). Potential Arctic tundra vegetation shifts in response to changing temperature, precipitation and permafrost thaw. *Biogeosciences*, *13*(22), 6229–6245. https://doi.org/10.5194/bg-13-6229-2016

Vishnivetskaya, T. A., Buongiorno, J., Bird, J., Krivushin, K., Spirina, E. V., Oshurkova, V., Shcherbakova, V. A., Wilson, G., Lloyd, K. G., & Rivkina, E. M. (2018). Methanogens in the Antarctic Dry Valley permafrost. *FEMS Microbiology Ecology*, *94*(8). https://doi.org/10.1093/femsec/fiy109

Wagner, D., & Liebner, S. (2010). Methanogenesis in Arctic permafrost habitats. In K. N. Timmis (Ed.), *Handbook of hydrocarbon and lipid microbiology* (pp. 655–663). Springer.

Walker, T. W. N., Kaiser, C., Strasser, F., Herbold, C. W., Leblans, N. I. W., Woebken, D., Janssens, I. A., Sigurdsson, B. D., & Richter, A. (2018). Microbial temperature sensitivity and biomass change explain soil carbon loss with warming. *Nature Climate Change*, *8*, 885–889. https://doi.org/10.1038/s41558-018-0259-x

Ward, C. P., & Cory, R. M. (2015). Chemical composition of dissolved organic matter draining permafrost soils. *Geochimica Et Cosmochimica Acta*, *167*, 63–79. https://doi.org/10.1016/J.GCA.2015.07.001

Wirsel, S. G. R. (2004). Homogenous stands of a wetland grass harbour diverse consortia of arbuscular mycorrhizal fungi. *FEMS Microbiology Ecology*, *48*(2), 129–138. https://doi.org/10.1016/j.femsec.2004.01.006

Wolf, A. A., Drake, B. G., Erickson, J. E., & Megonigal, J. P. (2007). An oxygen-mediated positive feedback between elevated carbon

dioxide and soil organic matter decomposition in a simulated anaerobic wetland. *Global Change Biology*, 13(9), 2036–2044. https://doi.org/10.1111/j.1365-2486.2007.01407.x

Woodcroft, B. J., Singleton, C. M., Boyd, J. A., Evans, P. N., Emerson, J. B., Zayed, A. A. F., Hoelzle, R. D., Lamberton, T. O., McCalley, C. K., Hodgkins, S. B., Wilson, R. M., Purvine, S. O., Nicora, C. D., Li, C., Frolking, S., Chanton, J. P., Crill, P. M., Saleska, S. R., Rich, V. I., & Tyson, G. W. (2018). Genome-centric view of carbon processing in thawing permafrost. *Nature*, 560(7716), 49–54. https://doi.org/10.1038/s41586-018-0338-1

Xiang, X., Wang, R., Wang, H., Gong, L., Man, B., & Xu, Y. (2017). Distribution of Bathyarchaeota communities across different terrestrial settings and their potential ecological functions. *Scientific Reports*, 7(1), 45028. https://doi.org/10.1038/srep45028

Yang, S., Liebner, S., Winkel, M., Alawi, M., Horn, F., Dörfer, C., Ollivier, J., He, J., Jin, H., Kühn, P., Schloter, M., Scholten, T., & Wagner, D. (2017). In-depth analysis of core methanogenic communities from high elevation permafrost-affected wetlands. *Soil Biology and Biochemistry*, 111, 66–77. https://doi.org/10.1016/j.soilbio.2017.03.007

Yashiro, Y., Sakai, S., Ehara, M., Miyazaki, M., Yamaguchi, T., & Imachi, H. (2011). *Methanoregula formicica* sp. Nov., a methane-producing archaeon isolated from methanogenic sludge. *International Journal of Systematic and Evolutionary Microbiology*, 61(Pt 1), 53–59. https://doi.org/10.1099/ijs.0.014811-0

Yoon, S.-H., Ha, S.-M., Kwon, S., Lim, J., Kim, Y., Seo, H., & Chun, J. (2017). Introducing EzBioCloud: A taxonomically united database of 16S rRNA gene sequences and whole-genome assemblies. *International Journal of Systematic and Evolutionary Microbiology*, 67(5), 1613–1617. https://doi.org/10.1099/ijsem.0.001755

Zona, D., Oechel, W. C., Kochendorfer, J., Paw U, K. T., Salyuk, A. N., Olivas, P. C., Oberbauer, S. F., & Lipson, D. A. (2009). Methane fluxes during the initiation of a large-scale water table manipulation experiment in the Alaskan Arctic tundra. *Global Biogeochemical Cycles*, 23, GB2013. https://doi.org/10.1029/2009GB003487

SUPPORTING INFORMATION

Additional supporting information may be found online in the Supporting Information section.